ADVANCED LINER COOLING NUMERICAL ANALYSIS FOR LOW EMISSION COMBUSTORS

A. Andreini *, J.L. Champion **, B. Facchini*, E. Mercier*, M. Surace***

***Department of Energy Engineering "Sergio Stecco" – University of Florence, Italy,**
**** LCD-CNRS, Poitiers France**
***** SNECMA, Villaroche, France**

Keywords:*liner, cooling, effusion*

Abstract

The aim to reach very low emission limits has recently changed several aspects of combustor fluid dynamics. Among them, combustor cooling experienced significant design efforts to obtain good performances with unfavourable conditions. This paper deals with simplified 1D and complete 3D conjugate numerical simulations of effusion cooling configurations, performed in the first two years of the European research project INTELLECT D.M. Geometries are derived from typical LPP combustor cooling configurations, which feature low coolant mass flow rate and high pressure losses (compared to typical blade cooling parameters).

Results are obtained in terms of local distributions of effectiveness and discharge coefficient. Comparison among simulations allowed to derive useful indications on overall effectiveness behaviour.

The configuration simulated in this paper represents a combustor liner with effusion cooling: the plate tested on the CNRS-LCD test rig of Poitiers is composed by two different patterns of effusion cooling. Furthermore, to be the most representative of a combustor chamber, an air flow bleed at the exit of the cold flow is introduced.

On the investigated plate SNECMA performed 3D conjugate (coupling fluid/thermal) calculations using a 3D CFD code named N3S-Natur and ABAQUS, a well known 3D thermal code. The codes take into account the effusion cooling area as an homogenous wall described by a permeability, a discharge coefficient for the CFD code and a convective flow (h_{con}, T_{con}) for the thermal one. That means that such simulations are not solving the flow inside each hole.

The fluid code also enables to compare the experimental adiabatic effectiveness measurements on this plate, but the aim is before all the overall effectiveness.

Conjugate calculations were also performed by means of a procedure employing 1D correlative fluid analysis and 2D metal conduction study. Finally, complete 3D CFD conjugated calculations has been carried out on the plate to verify the validity of assumptions and results obtained with simplified approaches previously exposed.

1 Introduction

Over the last ten years, there have been significant technological advances towards the reduction of emissions, strongly aimed at meeting the strict legislation requirements. Some very encouraging results have already been obtained but the reached solutions have created other technical problems. Modern aeroengine combustors, mainly LPP-DLN (Lean Premixed Prevaporized Dry Low NOx), operate with premixed flames and very lean mixtures, i.e. primary zone air amount grows significantly, while liner cooling air has to be decreased [1]. Consequently, important attention must be paid in the appropriate design of combustor liner cooling system; in addition, further goals need to be taken into account: reaction quenching due to cool air sudden mixing should be avoided, whilst temperature distribution has to reach the desired levels in terms of both pattern factor and profile factor

[2]. Among various possible techniques to guarantee an effective liner wall protection, effusion cooling certainly represents one of the most promising solutions. Effusion represents the evolution of classical film cooling solutions where the scheme is based on a limited number of injection rows, recently improved by the introduction of holes with very complex geometry, at least at the exit. Only in recent years, has the improvement of drilling capability allowed to perform a large amount of extremely small cylindrical holes, whose application is commonly referred as effusion cooling. Even if this solution does not guarantee, for each hole, the excellent wall protection achievable with film cooling, the most interesting aspect is the significant effect of wall cooling due to the heat removed by the passage of coolant inside the holes [3]. In fact, a higher number of small holes, uniformly distributed over the whole surface, permits a significant improvement in lowering wall temperature. From this point of view, effusion can be seen as an approximation of transpiration cooling by porous walls, with a slight decrease in performance but without the same structural disadvantages. Particularly for combustor liners, such solution appears very interesting because radiation contributes significantly to the heat flux, not sufficiently reduced by the film cooling alone. Studies on effusion cooling, or on multi-row hole injection have been performed to understand the complex phenomena which the effusion is based on, and experimental analysis appears fundamental [4, 5, 6, 7, 8, 9, 10]. The use of CFD is very complex for film cooling and particularly for effusion, because standard RANS (Reynolds Averaged Navier-Stokes Simulation) approach, with common turbulence models, is not able to reproduce correctly film effectiveness distribution, so more advances approaches as DES (Detached Eddy Simulation) or LES (Large Eddy Simulation) to solve Navier-Stokes equations are necessary [11, 12, 13, 14]. In the effusion cooling analysis, the conjugate approach to solve simultaneously heat convection and conduction appears very useful to better understand phenomena and to estimate cooling performances [15, 16, 17]. From the design point of view, the effusion requires a simulation tool in order to predict overall effectiveness, whenever boundary conditions and geometry parameters change. This could permit to properly design the hole array geometry depending on the location and the hot gas thermal loads. Such a tool can be developed basing on well known correlations about heat transfer inside the holes to predict film cooling adiabatic effectiveness [18, 19, 20, 21, 22]. The aim of this paper is to study a liner effusion cooling geometry comparing experimental analysis with CFD conjugate analysis, including some tests with the 1-D design tool. The objective of INTELLECT D.M. project is to develop a design methodology for lean burn low emission combustors to achieve a sufficient operability over the entire range of operating conditions whilst maintaining low NO_x emission capability. A specific work package inside the project is dedicated to the study of advanced liner cooling systems.

NOMENCLATURE

C	= CO_2 Concentration
Cd	= Effusion hole discharge coefficient
DP	= Pressure drop [Pa]
h	= Average heat transfer coefficient [W $m^{-2}K^{-1}$]
k	= Turbulent kinetic energy [m^2/s^2]
M	= Mach number
Re	= Reynolds number
p	= Pressure [Pa]
Q	= Mass flowrate [kg/s]
T	= Temperature [K]
x	= Streamwise distance [m]
y	= Distance for the plate [m]

Greeks

ε	= Turbulent dissipation [m^2/s^3]
ϕ	= Heat flux [W/m^2]
η	= Effectiveness
μ	= Viscosity [$kgm^{-1}s^{-1}$]
ρ	= Density [kg/m^3]

Subscripts

1st	= Grid first cell
1,2,3	= Section number
ad	= Adiabatic
aw	= Adiabatic wall
c	= Coolant
con	= Convective
g	= Gas
i	= Inlet, Input

h = referred to the holes
loc = local
ov = Overall
x = Abscissa in the streamwise direction
t = Turbulent
wall = Hot side wall

Superscripts

\+ = normalized

2 Experimental analysis

2.1 Test rig

The experimental study is performed using the THALIE test rig [23], whose schematic view is given in figure 1.

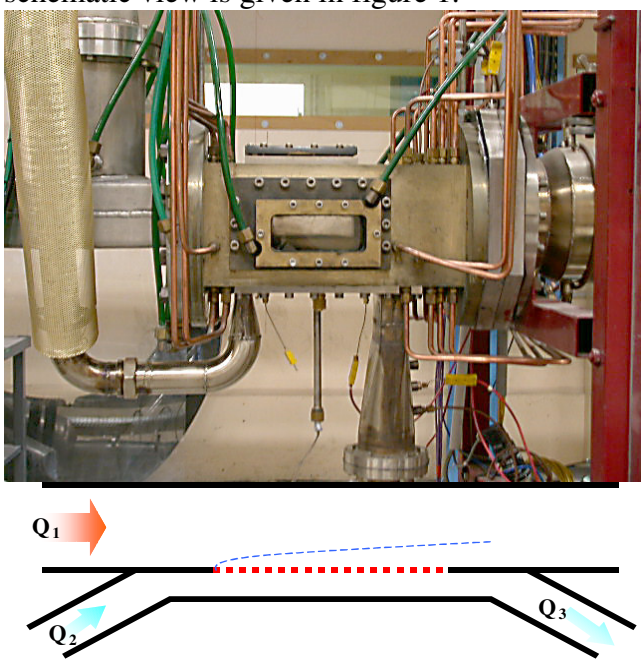

Figure 1: Schematic view of the experimental set up and of the THALIE's test section

THALIE allows aero-thermodynamical conditions close to those encountered in a combustor (T_1 up to 1200 K, T_2 up to 600 K). Primary burnt gases are generated by a tubular kerosene combustor and the secondary flow (coolant) is heated by an electrical heater. However, the present work has been carried out with T_2 = 273 K.

Main flow:		*subscript "1"*
	Cross section	123×72 mm²
	Reynolds number	$95000 < Re_1 < 272000$
Cooling flow:		*subscript "2"*
	Cross section	100×20 mm²
	Reynolds number	$5300 < Re_2 < 108000$
Hole flow:		*subscript "h"*
	Reynolds number	$0 < Re_h < 15000$
	Pressure ratio	Dp/p < 5%
	Mach number	$M_h < 0.2$

Table 1: Subscript 1 refers to the hot primary flow while subscript 2 refers to the secondary flow of cooling air

Available diagnostics are: Laser Doppler Velocimetry, optical measurements (Planar Laser Induced Fluorescence, Infra-Red Pyrometry), thin thermocouples, local gas analysis and flow visualizations. This metrology allows the determination of velocity, concentration and temperature inside the wall film as well as the wall temperature.

As shown in Figure 1, the combustor wall sample is placed in the rectangular test section, in such a way that hot burned gases (primary flow) and cooling air (secondary flow) are flowing parallel on each side of the solid separation. The variation ranges of the flow characteristics are given in table 1. Each of these parameters can be fixed independently and is monitored via PID controllers. This ensures reliability and reproducibility of the experimental conditions. Moreover, displacements of measurement devices and data acquisition are computer monitored.

P_1(Pa)	3 bar
T_1 (K)	1000 K
Q_1 (kg/s)	0.3
Re_1	56000
Q_2 (g/s)	0.1
T_2 (K)	273 K
Re_2 min / max	56000-75000

Table 2: Experimental conditions

2.2 Experimental conditions and procedures

Experiments have been carried out with T_1 close to 1000 K and T_2 close to 273 K The Reynolds number relative to the primary hot flow (Re_1) is fixed to 56000, while several values of Re_2 have been investigated. By changing the pressure loss step by step or continuously, the mass flow rate through the wall has been changed, allowing the

determination of Cd versus Re_h at fixed values of Re_1 and Re_2.

Experimental conditions are detailed in table 2. During all these experiments, the pressure loss remains lower than 5% to avoid compressibility effects inside holes. The Mach number (M_1) of the primary flow remains lower than 0.2. Mass flow rates (Q_1 and Q_2) are controlled by using PID controllers ensuring reliability and stability of the experimental conditions. Mass flow rates (Q_1, Q_2 and Q_3) are measured by Vortex flow-meters, the inaccuracy is less than 1%. Flow temperatures (T_1 and T_2) are measured by K-type thermocouples in the inlet section of the corresponding channels. The temperature T_2 results from the air expansion from the storage pressure (between 100 to 180 bar) to the atmospheric value. It is therefore subject to small changes during experiments. The static pressure (p_1) is measured by a transducer while the static pressure difference (Dp) is given by a differential transducer in the range 0-500 hPa. All these data (Q_1, Q_2, Q_3, T_1, T_2, P_1 and Dp) are acquired at the rate of 1 Hz and stored on a computer for post processing. Flow parameters (Re_1, Re_2, Re_h) are calculated using average values of measurements.

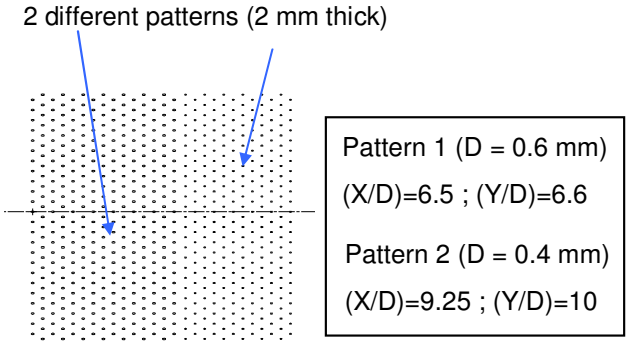

Figure 2: Experimental geometry

CO_2 concentration profiles at different streamwise locations have been performed normally to the wall by gas sampling. The knowledge of the wall CO_2 concentration (C_w) and the maximum CO_2 concentration measured inside the primary hot flow allows to calculate the non-dimensional wall CO_2 concentration $C^* = (C_1 - C_{loc})/C_1$. According to this latter expression, C* reaches its minimum value as the CO_2 concentration reaches its maximum. Finally, it must be noted that the value of C* at the wall gives the adiabatic cooling effectiveness $\eta_{ad} = (C_1 - C_{wall})/C_1$. The corresponding error on η_{ad} attached to this determination is found to remain lower than 5%.

Geometry is presented in figure 2.

3 Numerical calculations

3.1 SNECMA methodology

Considering the configuration of cooling system described before, CFD calculations have been performed to cross-check the experimental measurements of adiabatic effectiveness. The 3D CFD code used is N3S-Natur.

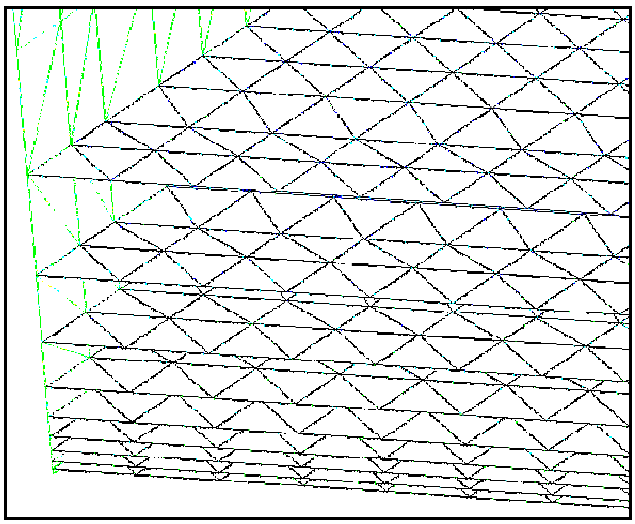

Figure 3: detail of boundary layer mesh

3.1.1 Calculation meshes

Two kinds of meshes have been realized for those calculations. The first one only takes into account the hot flow: the boundary condition of mass flow rate through the effusion cooling system is described thanks to an in-house 1D code.

The second mesh takes into account both flows. The CFD code, using a porosity condition, is able to calculate the mass flow rate through the effusion cooling system.

In order to have a good description of the wall laws, the meshes have been realized taking

into account a kind of boundary layer: the first layer is 0.2mm high (figure 3).

In figure 4 a complete view of both meshes is shown.

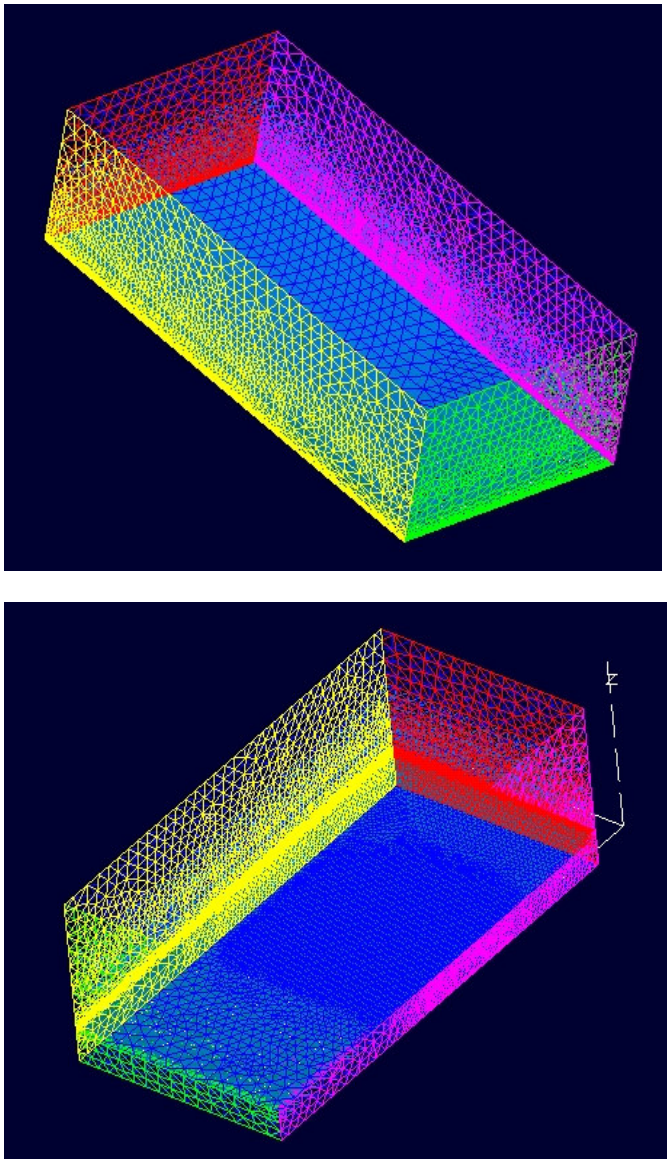

Figure 4: Overall view of calculation meshes used in SNECMA methodology

3.1.2 Boundary conditions

As previously said, the hot flow mesh need an in-house 1D code named GECOPE to impose the right mass flow rate through the effusion cooling system. Indeed, those two kinds of effusion cooling patterns have not the same description (holes diameter, distance between two rows especially). To couple the aerodynamic calculation with the thermal wall one, the boundary condition of effusion cooling also included a wall law.

The CFD code N3S-Natur needs different data to take into account the description of the effusion cooling:

- mass flow rate (only for the hot flow mesh)
- temperature
- permeability: holes area / total area
- discharge coefficient
- holes inclination
- turbulence (k, ε) (only for the hot flow mesh)

For all boundary conditions the turbulence rate has been taken equal to 5% and $\mu/\mu_t = 200$. That leads to k=2.5 and ε =70 for the hot entrance, and k=3.8 and ε=155 for the cold one.

3.1.3 Adiabatic effectiveness calculations

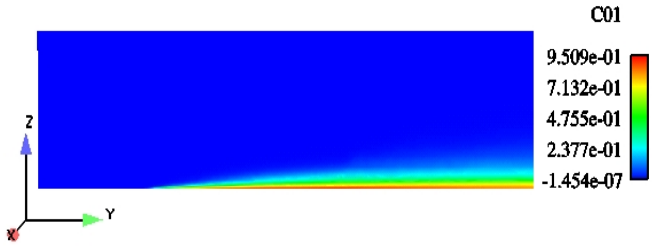

Figure 5: passive effluent field

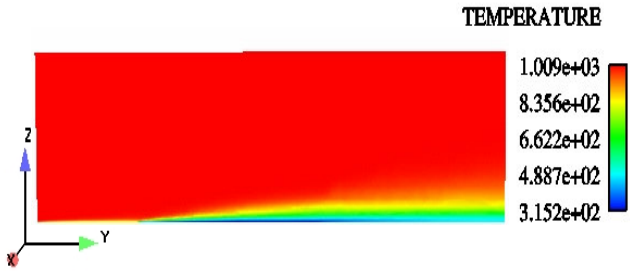

Figure 6: temperature field

Hot flow mesh calculations

Results are reported in terms of adiabatic effectiveness defined as:

$$\eta_{aw} = \frac{T_{aw} - T_g}{T_c - T_g} \qquad (1)$$

The adiabatic effectiveness is modeled using a passive effluent introduced for each effusion cooling boundary condition. We can see that the cold flow is well introduced and

enables to cool the air near the wall. Figures 5 and 6 show simulation results in terms of passive effluent and temperature fields.

Both flows calculations

The passive effluent that enables to follow the mixing of both flows through the effusion cooling is introduced at the cold entrance. Indeed, this condition calculates the mass flow rate through the effusion cooling and the mixing.

The global mass flow rate calculated is 37.1 g/s to compare with 39.6 g/s for the experimental measurements.

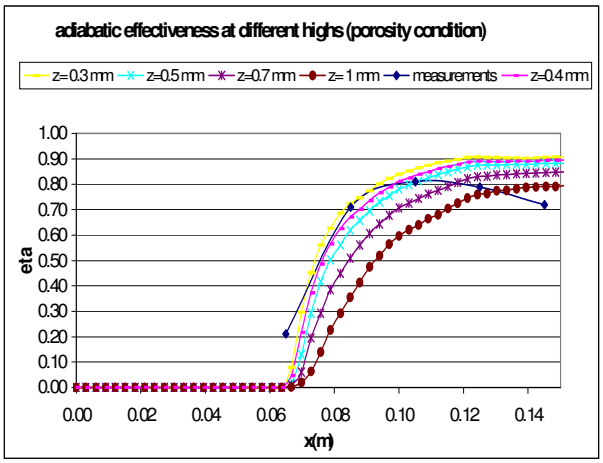

Figure 7: adiabatic effectiveness along the wall for porosity calculation

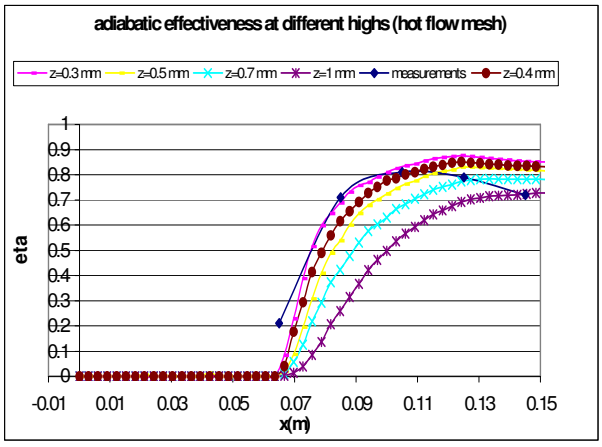

Figure 8: adiabatic effectiveness along the wall for hot flow mesh

The experimental measurements of the adiabatic effectiveness make use of a 0.5mm high probe that aspires the gas. To compare with the 3D calculations, we should post treat the calculations at different distances from the wall. Figures 7 and 8 show the η_{ad} distribution for both the calculation approach in comparison with experimental data.

The first measurement just after the second row of holes overestimates the cooling level because the sample is taken just behind an hole whereas the film cooling is not well developed.

The optimal distance from the wall is 0.3mm for both calculation.

3.1.4 Thermal calculations

Thanks to convective hot boundary conditions, a thermal calculation, using the code ABAQUS, has been performed. The great interaction between the CFD code and the thermal one is due to the formulation of the convective flux. Thus, iterative calculations have been performed to take into account this coupling.

Extraction of convective variables for the first iteration

The first calculation is adiabatic: $\phi_{wall} = 0$.

h_{con} is the convective coefficient, T_{con} the convective temperature and T_{aw} the adiabatic wall temperature. So:

$$\phi_{wall} = 0 \Rightarrow h_{con}(T_{aw} - T_{con}) = 0 \Rightarrow T_{con} = T_{aw} \quad (2)$$

So the convective temperature is equal to the adiabatic wall temperature.

A second calculation is done, by imposing a wall temperature of T_{con} + 100K.

$$\left.\begin{aligned} \phi_{wall} &= h_{con}(T_w - T_{con}) \\ &= h_{con}(T_{con} + 100 - T_{con}) \end{aligned}\right\} \Rightarrow \left\{ h_{con} = \frac{\phi_{wall}}{100} \right. \quad (3)$$

So the couple (h_{con}, T_{con}) is extracted from those 2 calculations.

Extraction of convective variables for others iterations

The same methodology could be used for others iterations:

$$\begin{cases} \phi_1 = h_{con}(T_{wi} - T_{con}) = 0 \\ \phi_2 = h_{con}(T_{wi} + X - T_{con}) = 0 \end{cases} \Rightarrow \begin{cases} h_{con} = \dfrac{\phi_2 - \phi_1}{X} \\ T_{con} = T_{wi} - \dfrac{X\phi_1}{\phi_2 - \phi_1} \end{cases} \quad (4)$$

Using directly the wall laws, we can extract the convective variables :

$$\Rightarrow \begin{cases} T_{con} = T_{1st} \\ h_{con} = \dfrac{\rho_p c_p u_f}{T^+} \end{cases} \qquad (5)$$

In figure 9 a temperature contour map for the last iteration is reported, while figures 10-12 describe the convergence of the overall methodology.

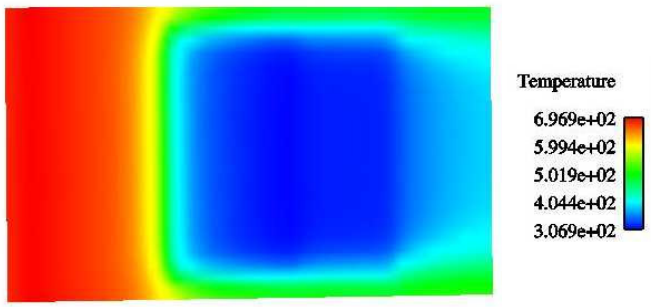

Figure 9: Hot side wall temperature at last iteration

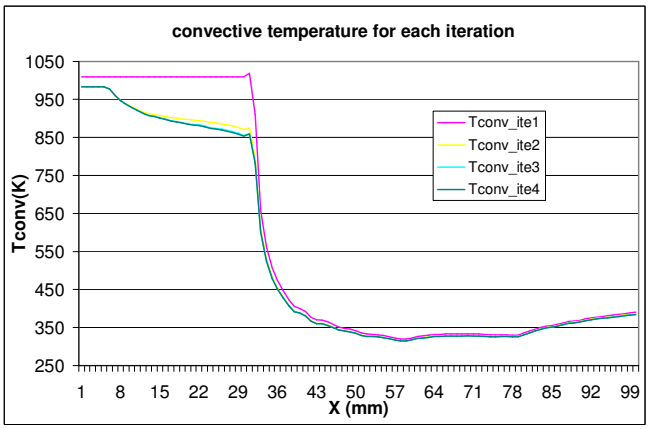

Figure 10: Convective temperature

We can notice that the convergence of the convective variables are fast and easy. We can consider that the third iteration is already converged.

3.2 Correlative approach

3.2.1 Description

In order to evaluate the accuracy of literature correlations employed in the preliminary design of film/effusion cooling systems, a correlative 1D procedure, coupled with a 2D FEM thermal solver, was set up.

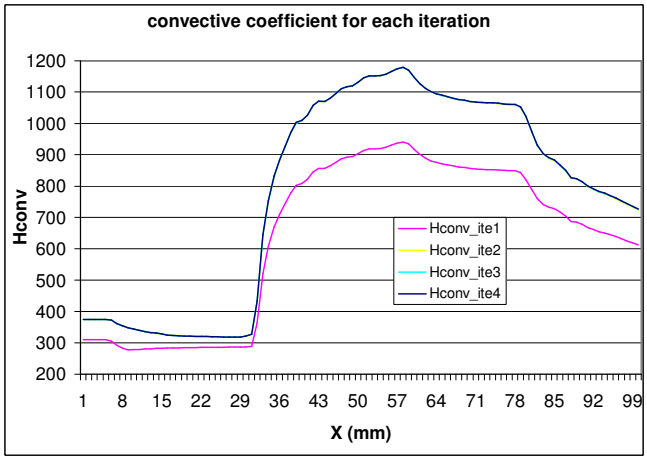

Figure 11: Convective coefficient

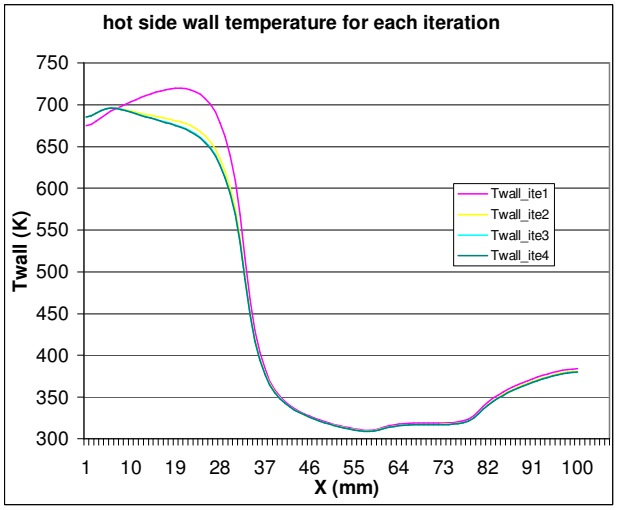

Figure 12: Hot side wall temperature

Such methodology allows to quickly evaluate the metal temperature distribution of a generic effusion cooled plate, so as to investigate wide variations of design parameters (hole spacing, angle, diameter) and boundary conditions. The procedure, which is described in details in [18,19], uses ANSYS™ as 2D FEM solver for thermal conduction within the flat plate. Hot and cold side boundary conditions (heat transfer coefficients and adiabatic wall temperatures) are obtained with standard fully turbulent smooth pipe correlations. Boundary conditions of effusion holes are evaluated by solving a 1D fluid network solver (SRBC code) which reproduces the main geometric features of actual geometry. Coolant is considered as a perfect gas subjected to wall friction and heat

transfer, which are evaluated with specific correlations: the flow field is solved in subsonic regime starting from boundary conditions specified at all inlets and outlets in terms of pressures or mass flow rates, depending on design specifications. Film cooling effectiveness on the hot side of flat plate is also calculated by SRBC code: in this case L'Ecuyer and Soechting [20] correlation was used to perform adiabatic film cooling effectiveness, while rows Seller's superposition, presented in Lakshiminarayana [24], is used. The overall interaction between SRBC code and ANSYS™, explaining the iterative procedure employed, is depicted in figure 13.

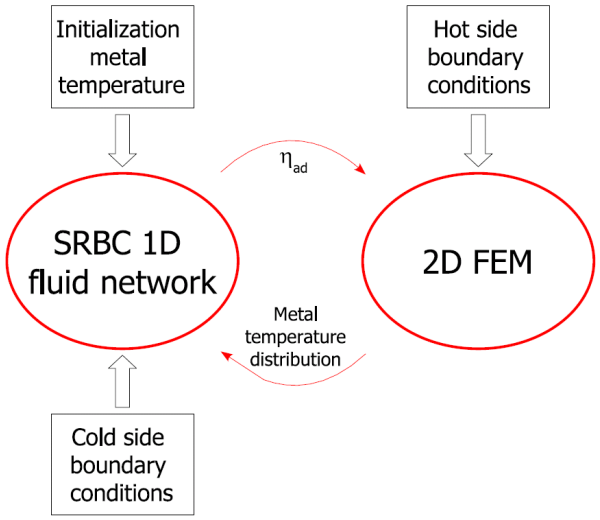

Figure 13: Flow diagram of 2D correlative procedure

Figure 14 reports a schematic description of the fluid network used for the analysis of the effusion cooled plate considered in this work.

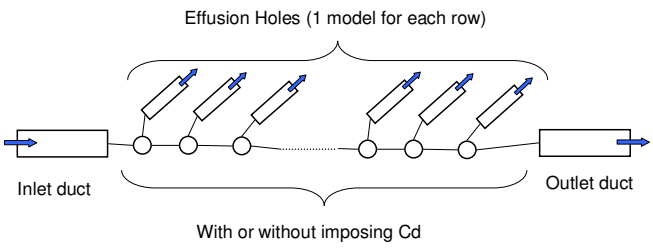

Figure 14: 1D fluid network

3.2.2 Results

The main source of uncertainty in this analysis is the evaluation of pressure losses due to effusion holes discharge and the estimation of heat transfer within the holes, which is responsible for the heat sink effect. In order to evaluate the impact on overall accuracy of these two matters, several simulations were performed with different assumptions:

1. Pressure losses in holes due to friction factor only
2. Pressure losses in holes due to friction factor plus an imposed discharge coefficient (Cd=0.9)
3. As in point 3 but using an heat transfer correlation specific for not fully developed pipes
4. Heat Sink effect neglected
5. Film cooling effect neglected (adiabatic effectiveness set to zero)
6. Pressure losses in holes estimated by imposing only a discharge coefficient, without wall friction (Cd=0.73)[21,22]

Flow boundary conditions were imposed as in experimental tests resulting in effusion cooling characteristics reported in table 3.

Effusion mass flow rate	0.937	kg/s
Discharge mass flow rate	0.06	kg/s
Blowing ratio	7.3	-
Velocity ratio	2.1	-

Table 3: Flow characteristic calculated by the fluid network model

Results are reported in terms of overall effectiveness, defined as:

$$\eta_{ov} = \frac{T_W - T_{Gas}}{T_{Cool\_in} - T_{Gas}}$$

Figure 15 depicts the distributions of overall effectiveness obtained with the six hypothesis above described.

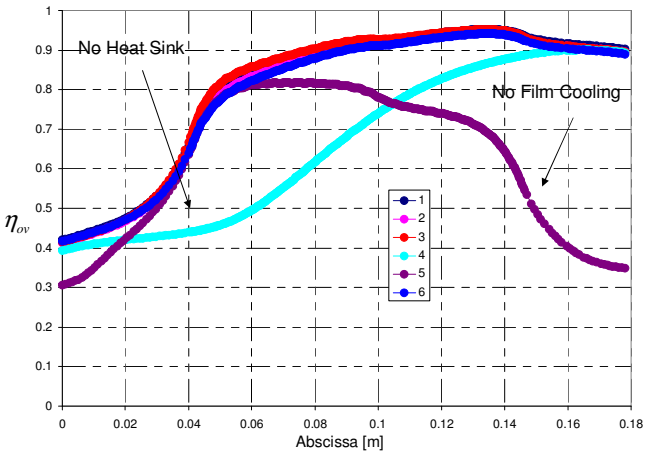

Figure 15 Overall Effectiveness distributions

First of all, it's important to point out the reduced influence of the criteria adopted for the analysis of pressure losses and heat transfer within the holes. Moreover, it's interesting to highlight the dominant contribution of heat sink effect in the first part of the plate, where film coverage is partial, with respect to the last part of the plate where the effect of reduction of the hot side adiabatic wall temperature prevails.

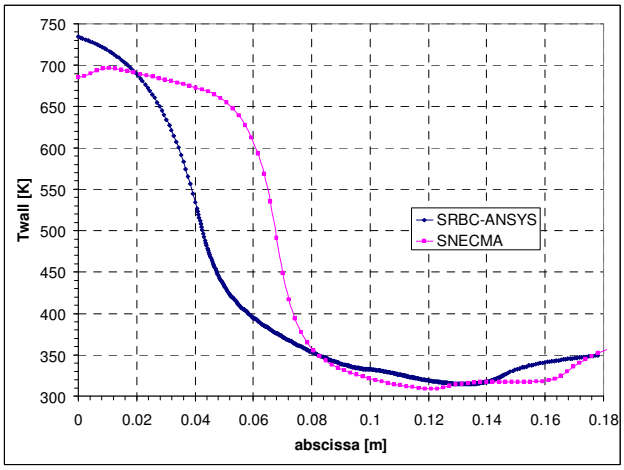

Figure 16 Hot side wall temperature vs. x direction

Figure 16 reports a direct comparison between hot side wall temperature predicted by SNECMA methodology and the correlative procedure above described. An overall good agreement is revealed especially in the last part of the plate where film cooling coverage dominates. The discrepancy in the first part of the plate, where heat sink effect prevails, is probably due to a different modeling of effusion holes: the distribution of heat sink effect adopted in SNECMA runs, probably neglect a smoothing effect to wall temperature which results in a steeper variation with respect to the correlative procedure.

3.3 Full 3D CFD conjugate analysis

As a final step in the analysis of the effusion cooled plate considered in this work, a full 3D CFD study was performed in order to obtain a detailed visualization of flow and temperature fields in the regions where the interaction between hot gas and coolant jets takes place.

3.3.1 Calculation tools and models

Calculations were performed using the industrial CFD code STAR-CD™, v. 3.26 developed and distributed by CD-Adapco. STAR is a finite volume unstructured solver with multi-physics capability (coupled solution of NS fluid equations and Fourier conductive equations). In this work fluid domain was solved using a compressible SIMPLE like algorithm, while flux discretization follows the Monotonic Advection and Reconstruction Scheme (MARS) for all the equations with the exception of continuity equation, where Central Differences were used. In order to assure a proper accuracy but keeping acceptable computational costs, a two equation k-ε model was selected, using a Two-Layer formulation for the near wall region (Norris and Reynolds scheme). Such approach requires about 15 cells within the boundary layer with a normalized distance for the first cell (y+) near unity for a proper discretization of the near wall zone,.

Calculation mesh was realized with an automatic multiblock structured approach, implemented in the STAR-CD preprocessor tool pro-STAR [17]. In order to keep mesh size below 4 millions elements (which approximately represents hardware limit) only the first eight rows of holes were considered. Figure 17 reports some details of computational mesh, while figure 18 describes the computational domain and its boundary conditions.

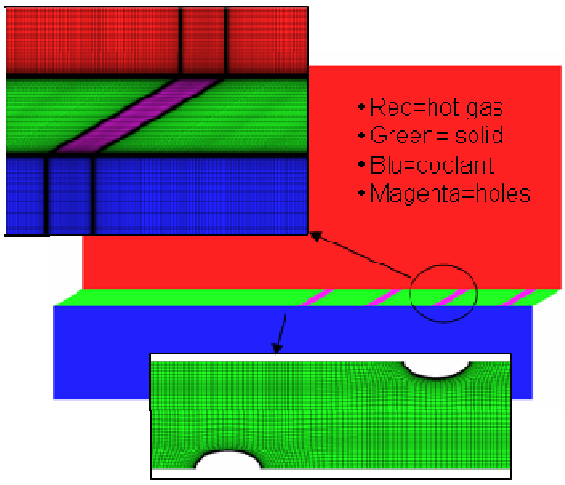

Figure 17: Details of calculation mesh (total 3.7 millions elements

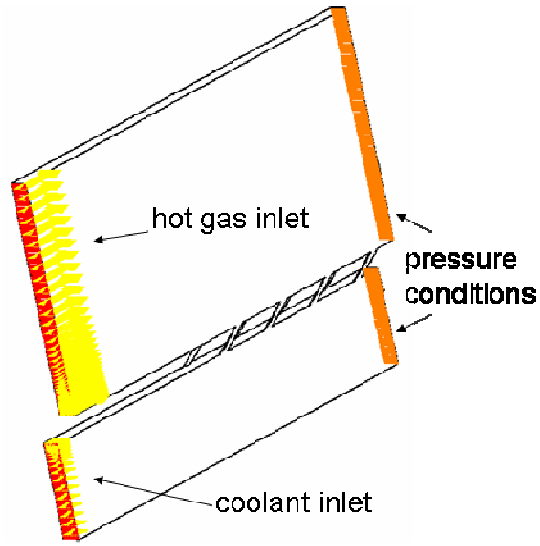

Figure 18: Computational domain and main boundary conditions

3.3.2 Results

Figure 19 compares adiabatic effectiveness results obtained by 3D CFD calculation and SRBC code with experimental data.

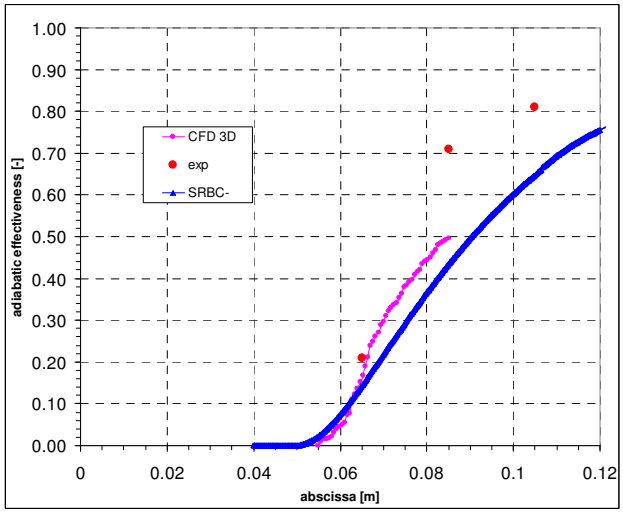

Figure 19: Axial distribution of laterally averaged adiabatic effectiveness vs. x direction

Spatial coordinate is limited to the range investigated with 3D CFD. Despite the known deficiencies of 2 equation turbulence models in the prediction of the spreading of round jets in cross flows [17], averaged effectiveness predicted by CFD calculations fairly agrees with correlation. On the other hand, experimental data are slightly under-predicted, but we have to consider that they are local values, sampled at different lateral positions.

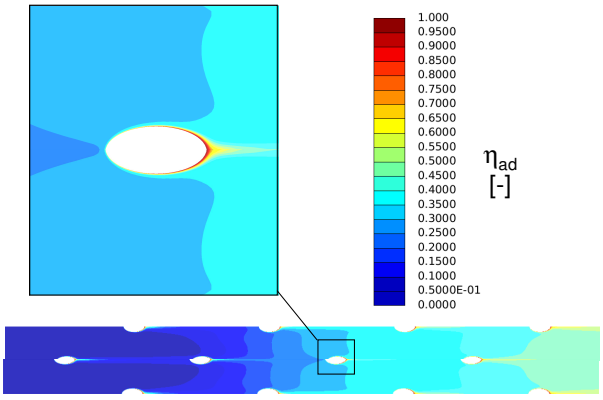

Figure 20: contour map of adiabatic effectiveness

A detailed contour map of adiabatic effectiveness is plotted in figure 20. Even if standard k-ε model tends to under estimate the spreading of round jets, it's important to point out how actual effectiveness distribution shows a visible non uniformity in lateral direction, which cannot be quantified with SNECMA methodology or correlative procedures.

Finally, some discussion about conjugate analysis. In order to keep a realistic heat flux as boundary condition on the metal side downstream of the last hole and upstream of the first one (see figure 21), the average temperature predicted with SRBC-ANSYS™ procedure was imposed.

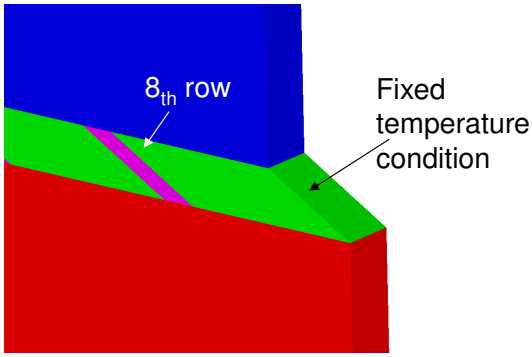

Figure 21: Detail of fixed temperature condition imposed at outlet metal side

Figure 22 compares overall effectiveness calculated with full 3D CFD and correlative procedure.

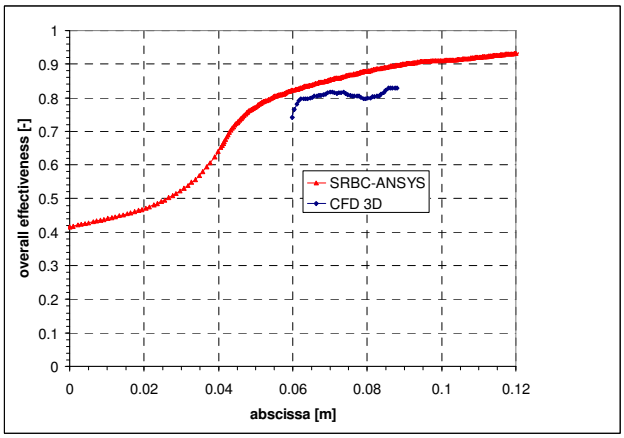

Figure 22: Overall effectiveness comparison

A good agreement is revealed confirming the validity of the assumptions. Figure 23 reports a detail of temperature field near a hole: the complex distribution depicted points out the importance of a 3D analysis during the design.

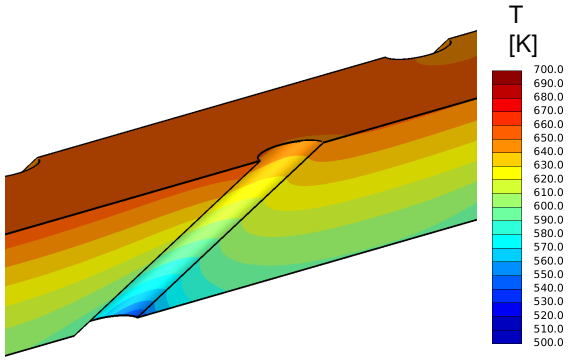

Figure 23 Temperature contours close the effusion hole predicted by conjugate analysis

4 Conclusions

The present study has investigated the cooling performance for a specific effusion configuration applied to a combustion chamber liner of a gas turbine aero-engine.

The analysis has focused on the comparison between experimental results and three different simulation approaches.

One correlative analysis based on 1-D/2-D model and two different solutions for a 3-D CFD approach have been compared.

The experimental adiabatic effectiveness distribution is fairly well predicted by all the numerical approaches as well as the coolant mass flowrate and discharge coefficient of perforated plate.

The overall effectiveness distribution has been calculated only by the three mentioned numerical approaches; only few limited discrepancies are noticeable, generally due to different hypotheses for the micro-holes modeling.

To sum up, the study shows the potentiality and the limits of the possible solutions for the effusion cooling numerical approach.

Acknowledgements

The present work was supported by the European Commission as part of FP6 STREP INTELELCT D.M. research program, which is gratefully acknowledged together with consortium partners.

References

[1] A. Schulz, *Combustor liner cooling technology in scope of reduced pollutant formation and rising thermalefficiencies*, Heat transfer in Gas Turbine Systems, 934, (2001), 135–146.)

[2] A. H. Lefebvre, *Gas Turbine Combustion*, Taylor & Francis (1998))

[3] K. M. B. Gustafsson. *Experimental studies of effusion cooling. Chalmers University of technology*, Department of Thermo and Fluid Dynamics, (www.tfd.chalmers.se/˜lada/postscript_files/bernhard_phd .pdf), 2001.

[4] Goldstein, R. J., Eckert, E. R. G., and Ramsey, J. W., 1968 *Film cooling with injection through holes: adiabatic wall temperatures downstream of a circular hole* J. of Engineering for Power, **90** , pp. 384.395.

[5] Afejuku, W. O., Hayi, N., and Lampard, D., 1979. *The film cooling effectiveness of double rows of holes*, ASME paper (79-GT/Isr-10) .

[6] M. Sasaki, K. Takahara, T. Kumagai, and M. Hamano. *Film cooling effectiveness for injection from multirow holes* Journal of Engineering for Power, **101**, 1979.

[7] R. E. Mayle and F. J. Camarata. *Multihole cooling film effectiveness and heat transfer* ASME Journal of heat transfer, **97**, 1975.

[8] G. E. Andrews, A. A. Asere, M. C. Mkpadi, and A. Tirmahi. *Transpiration cooling - contribution of film cooling to the overall cooling effectiveness* International Journal of Turbo and Jet Engines, **3**, 1986.

[9] G. E. Andrews, A. A. Asere, M. L. Gupta, and M. C. Mkpadi. *Effusion cooling: the influence of number of hole* Journal of Power and Energy, **204**, 1990.

[10] M. Martiny, A. Schulz, and S. Witting. *Full coverage film cooling investigations: adiabatic wall temperature and flow visualization* ASME Winter Annual Heat Transfer, (95- WA/HT-4), 1995.
[11] J. E. Mayhew, J. W. Baughn, and A. R. Byerley. *The effect of freestream turbulence on film cooling adiabatic effectiveness* ASME Turbo Expo, (GT-2002-30172), 2002.
[12] Leylek, J. H., and Zerkle, R. D., 1993. *Discrete-jet film cooling: A comparison of computational results with experiments* ASME Turbo Expo (93-GT-207) 2003.
[13] Roy, S., Kapadia, S., and Heidmann, J. D., 2003. *Film cooling analysis using des turbulence model* ASME Turbo Expo (GT-2003-38140), 2003.
[14] Acharya, S., and Tyagi, M., 2003, *Large eddy simulation of film cooling flow from an inclined cylindrical jet* ASME Turbo Expo (GT-2003-38633).
[15] Bohn, D., Ren, J., Kusterer, K., 2003, *Conjugate heat transfer analysis for film cooling configurations with different hole geometries* ASME Turbo Expo (GT2003-38369)
[16] Papanicolaou, E., Giebert, D., Koch, R., and Schulz, A., *A conservation-based discretization approach for conjugate heat transfer calculations in hot-gas ducting turbomachinery components*. International Journal of Heat and Mass Transfer, 44 , pp. 3413.3429, 2001.
[17] A. Andreini, C. Carcasci, S.Gori, M. Surace, 2005, *Film cooling system numerical design: adiabatic and conjugate analysis* ASME Heat Transfer Conference Expo (HT2005-72042)
[18] C. Carcasci, B. Facchini, G. Ferrara. *A rotor blade cooling design method for heavy duty gas turbine applications* ASME Cogen-Turbo Power, (95-CTP-90), 1995.
[19] C. Carcasci and B. Facchini. *A numerical procedure to design internal cooling of gas turbine stator blades*. Revue Generale de Thermique, 35, 1996.
[20] M. R. L'Ecuyer and F. O. Soechting. *A model for correlating flat plate film cooling effectiveness for rows of round holes*. AGARD Heat Transfer and Cooling in Gas Turbines (SEE N86-29823 21-07). September 1985.
[21] M. Gritsch, A. Schulz, and S. Wittig. *Method for correlating discharge coefficients of film cooling holes* AIAA Journal, 36, 1998.
[22] M. Gritsch, A. Schulz, and S. Wittig. *Discharge coefficient measurements of film cooling holes with expanded exits* ASME Journal of Turbomachinery, 120, 2001.
[23] Rouvreau, S., *Etude experimentale de la structure moyenne et instantane e d'un film produit par une zone multiperforee sur une paroi plane. Application au refroidissement des chambres de combustion de moteurs aeronautiques* PhD Thesis, CNRS, Poitiers, France 2001.
[24] B. Lakshminarayana,. *Fluid Dynamics and Heat Transfer of Turbomachinery*. John Wiley & Sons. New York, 1996.